Separating Intrinsic From Scattering Seismic Wave Attenuation From Sonic Logs in a Geothermal Field

Evert Durán[1], Kasper van Wijk[2], Ludmila Adam[1], and Irene Wallis[3]

[1]University of Auckland, School of Environment, Auckland, New Zealand
[2]University of Auckland, Department of Physics, Auckland, New Zealand
[3]Mighty River Power, Rotorua, New Zealand

Keywords

Ngatamariki, attenuation, sonic logging, radiative transfer, quality factor

ABSTRACT

Elastic waves attenuate in the earth due to scattering and absorption. The latter can be linked to fluid movement and is of the utmost importance to the production of a geothermal field. However, it is hard to separate scattering from intrinsic attenuation. Our approach is to use the full elastic waveform from borehole sonic logging, which consists of a coherent part, and incoherent signal produced by the scattered waves (coda). Based on the radiative transfer theory, the coherent energy is affected by the elastic wave attenuation due to both scattering and intrinsic attenuation, while scattering can provide a gain term in the incoherent energy. Here, we quantitatively analyse these intensities to independently estimate the quality factor due to scattering and absorption from full waveform sonic logs in a geothermal field.

Introduction

The analysis of elastic waves in the earth is often focused on estimates of the travel time (phase) of the first arriving compressional and/or transverse waves. However, seismologists now also analyze wave amplitudes to estimate the properties of the subsurface. One way to extract rock property information is to analyze the decay of seismic amplitude with distance; i.e., the loss of elastic energy due to elastic wave attenuation. Scattering attenuation is caused by heterogeneity in the earth, in the form of different rock materials, or in the presence of fractures. Intrinsic attenuation, or absorption, can be due to fluid movement as a result of a passing seismic wave. In field measurements, separating the loss of energy due to absorption versus scattering is difficult.

Wave attenuation is commonly described through the Quality Factor (Q) or its inverse (Q^{-1}) (Knopoff, 1964):

$$\frac{1}{Q} = \frac{\alpha v}{\pi f} \quad , \qquad \alpha = \frac{1}{x_2 - x_1} \ln \frac{A(x_1)}{A(x_2)} \tag{1}$$

where x_2 and x_1 are two different positions, $A(x_1)$ and $A(x_2)$ are the amplitudes measured at those positions and v and f are the velocity and frequency of the wave, respectively. The inverse of the quality factor provides a means of quantifying the dissipation of energy of the wave in a whole cycle of oscillation. The main factors affecting the value of Q summarized by Johnston (1981) and Müller et al. (2010) are: wave frequency, pore and confining pressures, fluid saturation, strain amplitude, fractures and rock composition (e.g. the degree of pore connectivity and mineralogic alteration). How these factors affect elastic wave propagation in rocks has been investigated in the laboratory for several decades (Birch (1960); Kern (1978); Toksöz et al. (1979); Batzle and Wang (1992); Punturo et al. (2005); Adam et al. (2009); Batzle et al. (2014)). Johnston et al. (1979) reviews some of the mechanisms acting at ultrasonic frequencies, concluding that friction, fluid flow, viscous relaxation and scattering are dominant. Müller et al. (2010) summarize the wave-induced fluid flow mechanisms (models) in the context of seismic wave attenuation. Understanding which are the main fluid and rock properties that control seismic wave attenuation is complicated. In deciding which attenuation mechanisms apply to field observations of Q, we would like to separate the scattering attenuation (Qs) from absorption (Qa).

Different methodologies have been proposed to estimate total attenuation from sonic logs (e.g. Cheng et al., 1982; Dasios et al., 2001; Parra et al., 2007). The most common methodology to estimate total Q from waveform data is by using spectral ratios of P-wave arrivals (Toksöz et al., 1979). However, Parra et al. (2007) point out that wave reflections and scattering can introduce oscillations in the amplitude spectra of the waveform, making it difficult to estimate Q from spectral ratios. In either case, the estimate of Q is the sum of scattering and intrinsic Q. Instead, We use elastic full waveform sonic data to estimate interval quality factors (Qs and Qa) with depth in a borehole. Our methodology focused on studying the energy produced by guided waves, and their scattering (i.e. coda). We first present a brief description of the full-waveform logging tool and common datasets. Next, we summarize the theory behind the radiative transfer theory. Finally, we present estimates of Qs and Qa and a preliminary interpretation for two wells in Ngatamariki Geothermal Field, New Zealand.

Radiative Transfer Theory

A wave is a perturbance of varying amplitude and phase in space and time. This perturbance, when performed over many realizations over the same medium, reveals systematic and fluctuating parts of the field; the coherent and incoherent field respectively. The square of the average wavefield $u(t)$ is known as the coherent intensity: $Ic = \langle u(x, t)\rangle^2$, whereas the average of the square of the wave fields is the total intensity $It = \langle u^2(x, t)\rangle$ (Ishimaru, 2013). The incoherent intensity of the field is the difference of the aforementioned intensities $Ii = It - Ic$. Radiative Transfer Theory describes the spatial and temporal dependence of the total intensity of seismic energy radiation in a particular direction (Paasschens, 1997). A quantitatively estimate of Qa and Qs offers an opportunity to identify sections where fluid movement is dominant (Van Wijk, 2003). The Radiative Transfer Theory provides an opportunity to separate scattering attenuation and absorption from full waveform log data based on the decay of the coherent and incoherent intensities of Stoneley waves in the borehole. The coherent ($C(x, t)$) and incoherent ($I(x, t)$) intensities according to the Radiative Transfer model in one dimension derived in Van Wijk (2003) and Haney et al. (2005) are:

$$I_c(x,t) \propto \exp\left(-\left(\frac{1}{l_a}+\frac{R}{l_s}\right)vt\right)\delta(x-vt),\ I_i(x,t) \propto \exp\left(-\left(\frac{1}{l_a}+\frac{R}{l_s}\right)vt\right)\left(I_0(\eta)+\sqrt{\frac{vt+x}{vt-x}}I_1(\eta)\right), \tag{2}$$

where $\eta = \frac{R}{l_s}\sqrt{(vt)^2 - x^2}$ with l_a the absorption mean free path, R/l_s the back-scattering cross-section (R), l_s the scattering mean free path, v the group – or energy – velocity, and t and x equal time and offset, respectively. I_0 and I_1 are the zero-th and first-order modified Bessel functions, and f is the frequency of the wave. In the following, we will find values of the scattering and absorption mean free paths that best fit the intensity data. Then, these mean free paths are related to the more familiar:

$$Q_a = \frac{2\pi f l_a}{v}\ , \qquad Q_s = \frac{2\pi f l_s}{v} \tag{3}$$

The Radiative Transfer Theory is implemented following a simple scheme. A common-offset section (ensemble) over a depth interval of interest is chosen and traces are stacked. Within this interval we estimate the total, coherent and incoherent intensity. The group velocity of the Stoneley wave for the ensemble stack is estimated from the coherent intensity of the 8 receivers. The coherent intensity and the incoherent intensity are fitted using equations 2 to estimate Qa and Qs as a function of depth in the borehole.

The Ngatamariki Geothermal Field

The Ngatamariki field has an installed electrical capacity of 82 MW. The field is located in the Taupo Volcanic Zone (TVZ) which is an area characterized by extensively faulted continental crust and a thick volcanic succession overlying a metasedimentary basement. The wells on the field are shown in Figure 1. Injection wells NM8 (north) and NM10 (south) contain a set of geophysical well logs. Wallis et al. (2009) describe the geophysical logging program conducted in 2012 at the Ngatamariki Geothermal Field in which a full waveform sonic log was acquired for well NM8. The full waveform data is a Dipole Shear Sonic Imager (DSI) recorded by Schlumberger. This dataset consists of a monopole source that generates a pulse traveling through the borehole fluid and into the geological formations. The tool records the waveforms at eight receivers separated six inches apart; where the first receiver is located nine feet from the monopole source. Full waveform sonic logs were collected in a pyroclastic section of well NM8 and in a deep andesite section in well NM10.

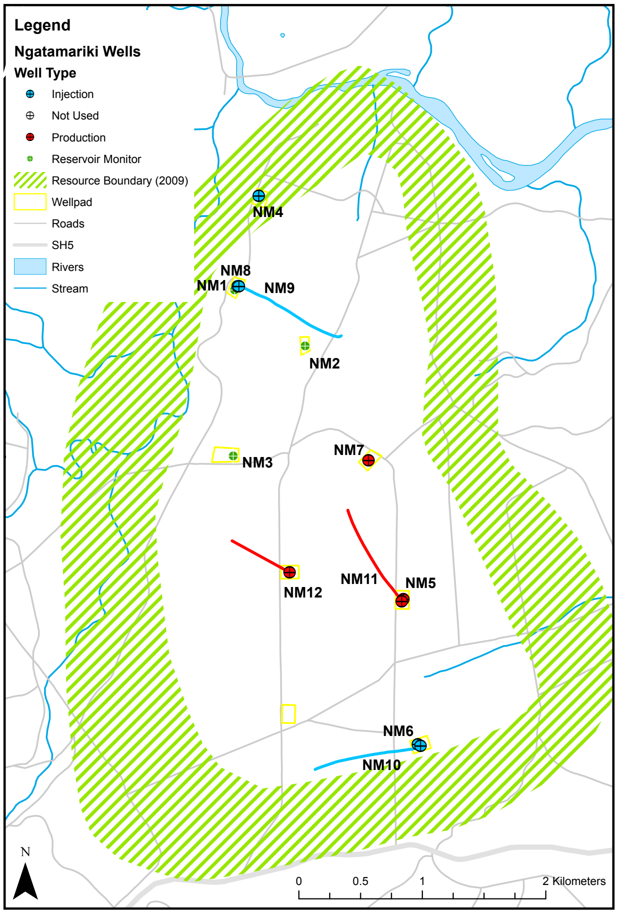

Figure 1. Location of the wells in the Ngatamariki geothermal field. Field boundaries are as given by Bibby et al. (1995).

Results and Discussion

The section of well NM8 logged by the DSI tool in Ngatamariki contains volcaniclastic and pyroclastic rocks mainly composed of tuff breccias and ignimbrites. We expect that attenuation of the sonic waves is dependent on the fractures and/or hydrothermal alteration in these rocks. Furthermore, in a geothermal setting we have the advantage of having only water as the saturating fluid. Thus, fluid viscosity effects on Q are potentially negligible with most of the variability in Q with depth resulting from rock permeability and fractures. The top panel of Figure 2 shows a typical shot gather of the DSI tool. One can clearly observe a coherent arrival of the Stoneley wave, which decays with offset. For each offset, the Stoneley wave is followed by scattered energy. The bottom panel displays an ensemble of 20 constant-offset traces from the first receiver. The blue lines in the panels of Figure 3 are the total, coherent and incoherent intensity for the ensemble of waveforms in Figure 2. The red lines are the best fits to the different intensities, where a value of R = 0.5 was assumed for the backscattering cross-section (R); this implies for the 1D model assumed here that energy transmits and reflects equally at the scatterers within the ensemble. The group velocity v of the Stoneley arrivals is estimated from the move-out of the peak of the total intensity as a function of source-receiver offset. With these values, the fits shown are for values of the absorption mean free path (*la* = 1 m) and the scattering mean free path (*ls* = 0.55 m) were estimated, which results in Qa = 59 and Qs = 33.

Figure 4 shows the estimated values of Qa and Qs for the well NM8, which we believe correlate with geology. For example, Qa estimates are lower in the zones of washouts. A decrease in Qa (i.e., stronger attenuation) between 1390 m and 1405 m is accompanied by a decrease in resistivity. This is likely indicating a region of favorable mobility for fluids. Below this, estimates of Qa show an abrupt increase (lower attenuation) and higher variability. Geologically, this area corresponds to a welded ignimbrite. In this section, the resistivity increases, indicating less porosity and hence a higher level of compaction. The effect of the lithologies and their different levels of compaction and alteration must be evaluated in detail. Lower values of Qs than Qa seem to indicate that most of the attenuation is probably due to scattering in the borehole. The scattering attenuation estimates Qs show also less variability than Qa. The total value of Q is given by the combination of absorption (Qa) and scattering (Qs); when scattering is as strong as shown here, the absorption component related to fluids is almost completely masked. The separation of quality factors achieved by the radiative transfer model appears to overcome this difficulty.

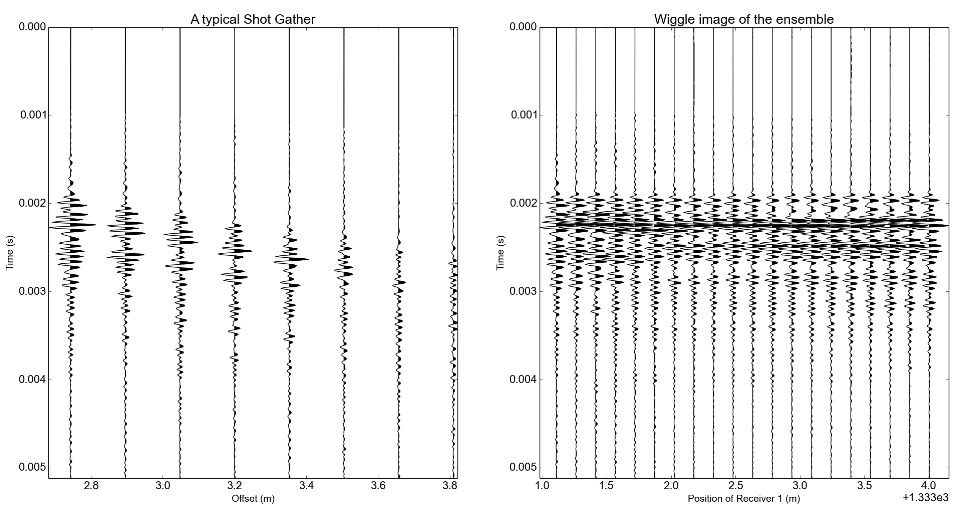

Figure 2. Typical shot gather (left) and ensemble made of the waveforms recorded by the first receiver in well NM8 (right). Each waveform is separated by a half-foot distance. The ensemble shown on the right panel is made of 20 waveforms, covering a section of around 3 m. The total recorded time is 5.12 ms at a sampling rate of 10 ms.

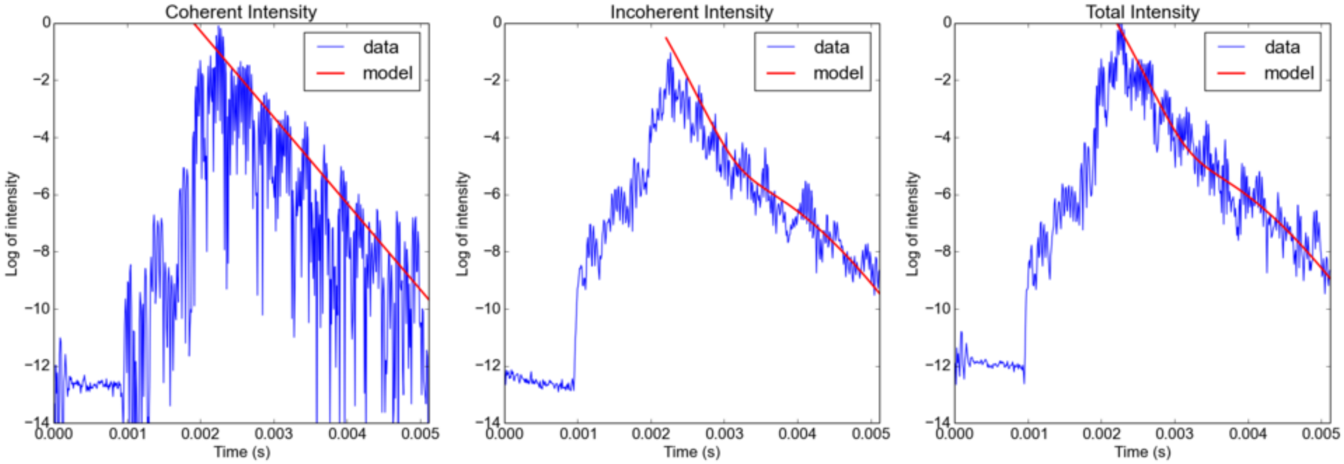

Figure 3. Wave intensities calculated from the ensemble of traces shown in Figure 2. From left to right: coherent, incoherent and total intensity. The values of Qa and Qs obtained for this fits are 59 and 33, respectively. The absorption mean free path (la) is 1 m while the scattering mean free path (*ls*) for a back-scattering cross-section R = 0.5 is 0.55 m.

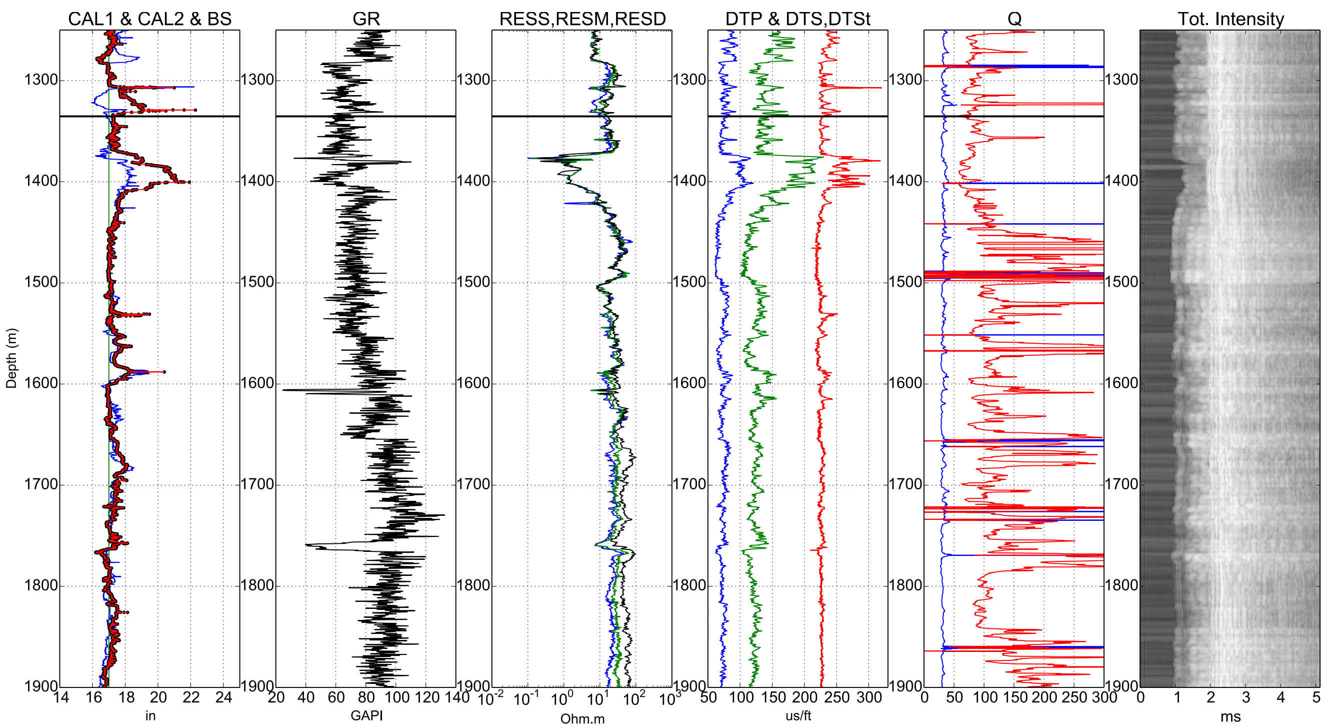

Figure 4. Geophysical well logs of the well NM8. The wash-out areas are those where the caliper logs read a greater borehole diameter than the bit size (17 in). The slowness logs correspond to the P-wave (DTP), S-wave (DTS) and Stoneley wave (DTSt). GR is the gamma ray log, RESS, RESM, RESD are resistivity logs. Qa (red) and Qs (blue) are estimated from an ensemble of 20 first receivers using the monopole source data. The black line at 1334 m marks the depth at which the intensities shown before were fitted.

Well NM10

The logged part of well NM10 corresponds to the Ngatamariki Andesite. This andesite has a high number of conductive fractures (Halwa, 2012). Figure 5 shows the correlation between absorption (Qa) and FMI fracture density interpretation for the top section of the andesite (this section has the highest quality sonic data). The plot shows only conductive fractures with no halo, which are interpreted as open or clay-filled fractures (Halwa, 2012). A preliminary correlation between low absorption (high attenuation) and higher fracture density can be observed. Open fractures in rocks are responsible for the losses in wave energy due to pore pressure disequilibrium created by the passing wave (Pride et al., 2004).

High Qa (low attenuation) overall correlates to sections where fracture density is low. Although the correlations between Qa values and fracture density is generally strong, a lack of correlation in some parts can be due to 1) clay-filled fractures that contribute to the fracture density would not affect Qa, or 2) FMI images have a lower resolution of 5 mm, however these micro-fractures will still affect the flow properties and attenuation of waves. Although the technique presented here has been applied to volcanic rocks, we believe this methodology and our findings can be equally applied to carbonate fractured rocks and/or high permeable sandstone reservoirs.

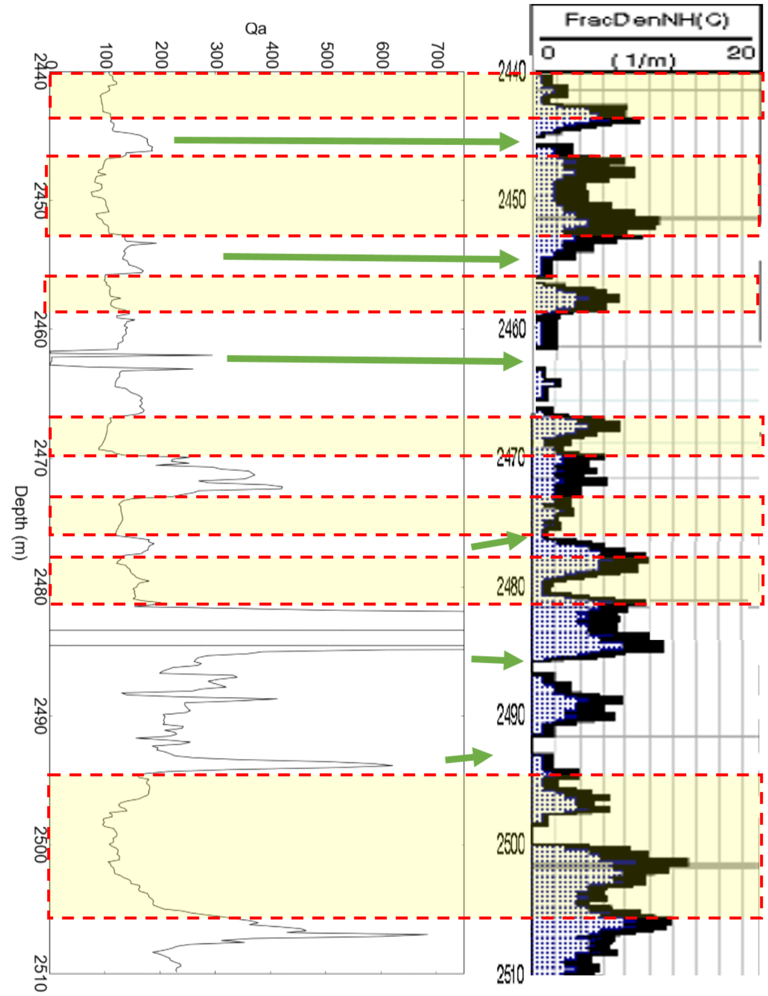

Figure 5. Preliminary interpretation of absorption Q on the upper andesite section at Ngatamariki (Well NM10). Fracture density log from (Halwa, 2012). The dashed square areas show the matches between the variations of Qa with the fracture density log.

References

Adam, L., M. Batzle, K. Lewallen, and K. Van Wijk, 2009, Seismic wave attenuation in carbonates: Journal of Geophysical Research: Solid Earth, 114.

Batzle, M., G. Kumar, R. Hofmann, L. Duranti, and L. Adam, 2014, Seismic-frequency loss mechanisms: Direct observation: The Leading Edge, 33, 656–662.

Batzle, M., and Z.Wang, 1992, Seismic properties of pore fluids: Geophysics, 57, 1396–1408.

Bibby, H. M., T. G. Caldwell, F. J. Davey, and T. H. Webb, 1995, Geophysical evidence on the structure of the Taupo Volcanic Zone and its hydrothermal circulation: Journal of Volcanology and Geothermal Research, 68, 29–58.

Birch, F., 1960, The velocity of compressional waves in rocks to 10 kilobars, Part 1: Journal of Geophysical Research, 65, 1083–1102.

Cheng, C., M. Toksöz, and M. Willis, 1982, Determination of In Situ Attenuation from Full Waveform Acoustic Logs: Journal of Geophysical Research, 87, 5477–5484.

Dasios, A., T. R. Astin, and C. McCann, 2001, Compressional wave Q estimation from full-waveform sonic data: Geophysical Prospecting, 49, 353–373.

Halwa, L., 2012, Image Interpretation Report (FMI & AFIT). Mighty River Power Ngatamariki-10: Technical report, Schlumberger.

Haney, M. M., K. van Wijk, and R. Snieder, 2005, Radiative transfer in layered media and its connection to the o'doherty-anstey formula: Geophysics, 70, T1–T11.

Ishimaru, A., 2013, Wave propagation and scattering in random media: Elsevier Science.

Johnston, D., M. Toksöz, and A. Timur, 1979, Attenuation of seismic waves in dry and saturated rocks: II. Mechanisms: Geophysics, 44, 691–711.

Johnston, D. H., 1981, Attenuation: A state-of-the-art summary, in Seismic Wave Attenuation: SEG, Geophysics reprint series No.2.

Kern, H., 1978, The effect of high temperature and high confining pressure on compressional wave velocities in quartz-bearing and quartz-free igneous and metamorphic rocks: Tectonophysics, 44, 185–203.

Knopoff, L., 1964, Q: Reviews of Geophysics, 2, 625–660.

Müller, T., B. Gurevich, and M. Lebedev, 2010, Seismic wave attenuation and dispersion resulting from wave-induced flow in porous rocks a review: Geophysics, 75, 75A147–75A164.

Paasschens, J. C. J., 1997, Solution of the time-dependent Boltzmann equation: Phys. Rev. E, 56, no. 1, 1135–1141.

Parra, J. O., P. C. Xu, and C. L. Hackert, 2007, A borehole model-derived algorithm for estimating Qp logs from fullwaveform sonic logs: Geophysics, 72, E107–E117.

Pride, S. R., J. G. Berryman, and J. M. Harris, 2004, Seismic attenuation due to wave-induced flow: Journal of Geophysical Research: Solid Earth (1978–2012), 109.

Punturo, R., H. Kern, R. Cirrincione, P. Mazzoleni, and A. Pezzino, 2005, P- and S-wave velocities and densities in silicate and calcite rocks from the Peloritani Mountains, Sicily (Italy): The effect of pressure, temperature and the direction of wave propagation: Tectonophysics, 409, 55–72.

Toksöz, M., D. Johnston, and A. Timur, 1979, Attenuation of seismic waves in dry and saturated rocks: I. Laboratory measurements: Geophysics, 44, 681–690.

Van Wijk, K., 2003, Multiple scattering of surface waves: PhD thesis, Colorado School of Mines.

Wallis, I., S. McCormick, S. Sewell, and C. Boseley, 2009, Formation assessment in geothermal using wireline tools – application and early results from the Ngatamariki geothermal field, New Zealand: Presented at the 31st New Zealand Geothermal Workshop.